Delta University Scientific Journal
Journal home page: https://dusj.journals.ekb.eg

1,2,3,4-Tetrahydropyrimidine-clubbed quinoline hybrid: Radiolabeling, Biodistribution and Imaging

Basem Mansour[1,2]*, Mennat A. Sherif[1], Ismail. T. Ibrahim[3,4], Magda A. El-Sayed[5,6], Mohammed A. M. Massoud[5], Waleed A. Bayoumi[5]

[1]*Department of Pharmaceutical Chemistry, Faculty of Pharmacy, Delta University for Science and Technology, Gamasa 35712, Dakahlia, Egypt*
[2]*Department of pharmacy, Kut University College, Al Kut 52001, Wasit, Iraq.*
[3]*Labeled comp department, Hot lab center, Egyptian Atomic Energy Authority, Cairo 13759, Egypt.*
[4]*Department of pharmacy, Al-Huda University college, Ramadi 31001, Al Anbar, Iraq*
[5]*Department of Pharmaceutical Organic Chemistry, Faculty of Pharmacy, Mansoura University, Mansoura 35516, Egypt.*
[6]*Department of Pharmaceutical Chemistry, Faculty of Pharmacy, Horus University, New Damietta, 34518, Egypt.*

Correspondence: Basem Mansour; Department of Pharmaceutical Chemistry, Faculty of Pharmacy, Delta University for Science and Technology, Gamasa 35712, Dakahlia, Egypt; Tel : +2 050 277 0140; Fax +2 050 277 0145; Email : basem2412@yahoo.com

ABSTRACT

Cancer represents a broad category encompassing various diseases that can impact any area of the body. It is also referred to as malignant tumors or neoplasms. Aiming to diagnose tumors, a promising monastrol analogue (**1b**) methyl 4-(2-hydroxyquinolin-3-yl)-6-methyl-2-oxo-1,2,3,4-tetrahydropyrimidine-5-carboxylate, was designed *via* structural modification of monastrol, and synthesized in good yield. This compound was *in vitro* evaluated *via* MTT assay and revealed potent antitumor effects on a panel of cancer cell lines namely; HepG-2, HCT-116, MCF-7, and PC3 against standard 5-fluorouracil. The target **1b** was radiolabeled with iodine-131 by a direct electrophilic substitution reaction. It was found that ^{131}I-**1b** has a high radiolabeling yield (96.40 ± 2.00%), stability, solid tumor uptake, and Target/Non-target ratio (T/NT) ratio (5 ± 0.03 at 30 min. post-injection) compared with many new tracers which have been developed in recent years. This study encourages the possible use of this tracer as a potential imaging and/or therapeutic agent for cancer.

Keywords: *Monastrol; Quinolines; Dihydropyrimidin-2(1H)-one; Radioiodination; Tumor.*

1. Introduction

Cancer represents a broad category encompassing various diseases that can impact any area of the body. It is also referred to as malignant tumors or neoplasms. A hallmark characteristic of cancer is the swift proliferation of atypical cells that exceed their normal limits and can infiltrate neighboring body parts and migrate to other organs (metastasis). The majority of cancer-related deaths are due to extensive metastases (Bray et al., 2018; Xu et al., 2008).

Quinoline ring, 1-aza-naphthalene or benzo[*b*]pyridine as a bicyclic heterocyclic system, comprises pyridine and benzene rings fused to each other by adjacent carbons (Dobbin, 1934) so it is considered a nitrogen-containing heterocycle and functional intermediates in organic synthesis. Being a tertiary amine, the quinoline ring can form a salt with acids and displays both electrophilic and nucleophilic aromatic substitution reactions, and it or its derivatives have natural as well as synthetic sources (Matada, Pattanashettar, Yernale, & Chemistry, 2021). Quinolines play a crucial role in medicine, forming the backbone of many drugs for treating many disease conditions including schistosomiasis associated with hepatic fibrosis (El-Barabry et al., 2021), acute and chronic toxoplasmosis as a single therapy (Abd Elgawad et al., 2019) or combined with nitazoxanide (Elblihy et al., 2024; Youssef & El Ganyny), epilepsy (El-Gamal et al., 2022), Alzheimer (Li et al., 2023), hypertension (Patil, Padmashal, & Uppar), and cancer (Chu et al., 2019; Fujioka et al., 1992; B. Mansour, Bayoumi, El-Sayed, Abouzeid, & Massoud, 2022; B. Mansour, Henen, Bayoumi, El-Sayed, & Massoud, 2021; B. Mansour et al., 2023; Massoud, El-Sayed, Bayoumi, & Mansour, 2019). Furthermore, quinoline-based compounds were ubiquitously used as anti-inflammatory and analgesic (Ghanim et al., 2022), antiviral (Wang et al., 2021), anti-bacterial and anti-fungal (Sharma & Singh, 2022).

However, another nitrogen-based heterocycle is the functionalized 3,4-dihydropyrimidin-2(1*H*)-one (DHPM) ring. DHPM which was first reported by the Italian chemist Petro Biginelli (Biginelli, 1893) *via* a three-component condensation reaction of an aromatic aldehyde, urea, and ethyl acetoacetate, is a doubly unsaturated six-membered ring and has two nitrogen atoms at positions 1 and 3. Soon after its first report, DHPM ring became one of the most important and desirable scaffolds in medicinal chemistry due to its diverse biological activities such as anti-inflammatory and analgesic (Dawood, Jasass, Amin, Farghaly, & Abbas, 2017), antibacterial (Cui et al., 2017), antioxidant (Ergan et al., 2017), antihypertensive activities (Teleb et al., 2017), antifungal (de Azambuja et al., 2019), antiviral (Ma et al., 2021), and anticancer (El-Azab, Abdel-Aziz, Ghabbour, Al-Gendy, & Chemistry, 2017; Ragab, Abou-Seri, Abdel-Aziz, Alfayomy, & Aboelmagd, 2017). Moreover, a recently prepared series of 3,4-dihydropyrimidines was reported to possess significant antiproliferative activity and anti-breast cancer cytotoxicity (Sośnicki et al., 2014).

The early and accurate diagnosis of tumors will intensively improve the treatment plans for the patients. In an effort to increase patient survival and improve prognoses, the development of tumor diagnosis and treatment agents is important (M. Motaleb, Abdel-Ghaney, Abdel-Bary, & Shamsel-Din, 2016). Radioiodinated compounds are widely used for the diagnosis and treatment of tumors e.g. [^{125}I]-iodothioguanine for cancer treatment (Saleh-Abady et al., 2010) and [^{123}I]-iodocelecoxib for tumor imaging (Saleh-Abady et al., 2010). Most nuclear medicine

departments use single-photon emission computed tomography (SPECT) as one of their standard technologies (Ibrahim et al., 2015; Sakr, Essa, El-Essawy, & El-Mohty, 2014).

Recently, studies have focused on radiopharmaceuticals containing technetium-99m and radioiodine to be used for targeting solid tumors (M. Motaleb et al., 2016). The development of new radiopharmaceuticals, which target specific receptors in solid tumors, could potentially have high tumor uptake and high solid tumor to normal muscle (T/NT) ratio which results in potential diagnostic radiopharmaceuticals with a high quality (M. Motaleb et al., 2016).

2. Material and methods

2.1. Chemistry

Methyl 4-(2-hydroxyquinolin-3-yl)-6-methyl-2-oxo-1,2,3,4-tetrahydropyrimidine-5-carboxylate (**1b**) was synthesized according to the previous report (B. A. Mansour, El-Sayed, Massoud, & Bayoumi, 2024).

2.2. Radioiodination procedure

Different amounts of substrates (10–250 μg) in dimethyl sulfoxide (DMSO) were added to an amber color vial. Then, 170 μL of freshly prepared chloramine-T (CAT) solution in ethanol containing (10–250 μg) CAT was added. Then, 10 mL of $Na^{131}I$ (7.2 MBq) was added to the reaction mixture and pH was adjusted by using 150 μL buffer solutions. The reaction mixture was vortexed and left at ambient temperature for 5–60 min. A drop of saturated sodium thiosulfate solution (10 mg/mL H_2O) was added to decompose the excess of iodine (I_2) in order to quench the reaction by reducing it to iodide (I^-) as it is oxidized to tetrathionate ($S_4O_6^{2-}$) (Kurth, Dahl, & Butt, 2015). The effect of various reaction parameters and conditions on radioiodination efficiency, such as the amount of oxidizing agent (CAT), amount of substrate, pH of the reaction, and the reaction time were optimized in order to maximize the radiochemical yield.

2.3. Tumor transplantation

Ehrlich Ascites Carcinoma (EAC) as a model in cancer research was used in this work. EAC was maintained in female Swiss albino mice through weekly intraperitoneal (IP) transplantation (Ozaslan, Karagoz, Kilic, & Guldur, 2011). EAC cells were obtained by needle aspiration under aseptic conditions. The ascetic fluid was diluted with sterile saline (0.1 mL contains 2.5×10^6 cells) then 0.1 mL of this solution was injected into the peritoneal cavity of mice to produce liquid tumor and intramuscularly in the muscle of the right leg of the mice to produce solid tumor keeping left leg as control. Mice were kept for 7 to 10 days on a normal diet in a metabolic cage till the tumor was observed.

2.4. Biodistribution of ^{131}I-1b

Biodistribution assay was carried out in normal and tumor-bearing (ascites and solid) mice. Each group consisted of 16 mice divided into 4 subgroups (4 mice each). Injection of 0.2 mL **(**74 KBq) of ^{131}I-**1b** was done via mice tail vein. Mice were sacrificed at 15, 30, 60, and 120 min by cervical dislocation after anesthesia with chloroform. Organs and fluids of interest were removed, weighed, and counted in a gamma scintillation counter to determine their uptake of ^{131}I-**1b**. Samples of blood and organs of interest were removed, weighed, and assayed for

radioactivity, and the percentages of injected dose per gram (% ID/ g) were calculated. Bone, blood, and muscle weight were taken as 10, 7, and 40% of the total body weight, respectively (M. Motaleb, Selim, El-Tawoosy, Sanad, & El-Hashash, 2017). Solid tumor to normal muscle (T/NT) was calculated.

3. Results and Discussion

3.1. Radiolabeling study

Several Monastrol derivatives (**1a-i**) (Figure 1) were selected for radioiodination *via* electrophilic substitution reaction with radioactive iodine-131 and chloramine-T (CAT) as an oxidizing agent. Out of the tested compounds, compound **1b** showed the highest radiochemical yield (96.40 ± 2.00%) and has been promoted for further biological investigation. Several parameters affect the process of radiolabeling, as follows:

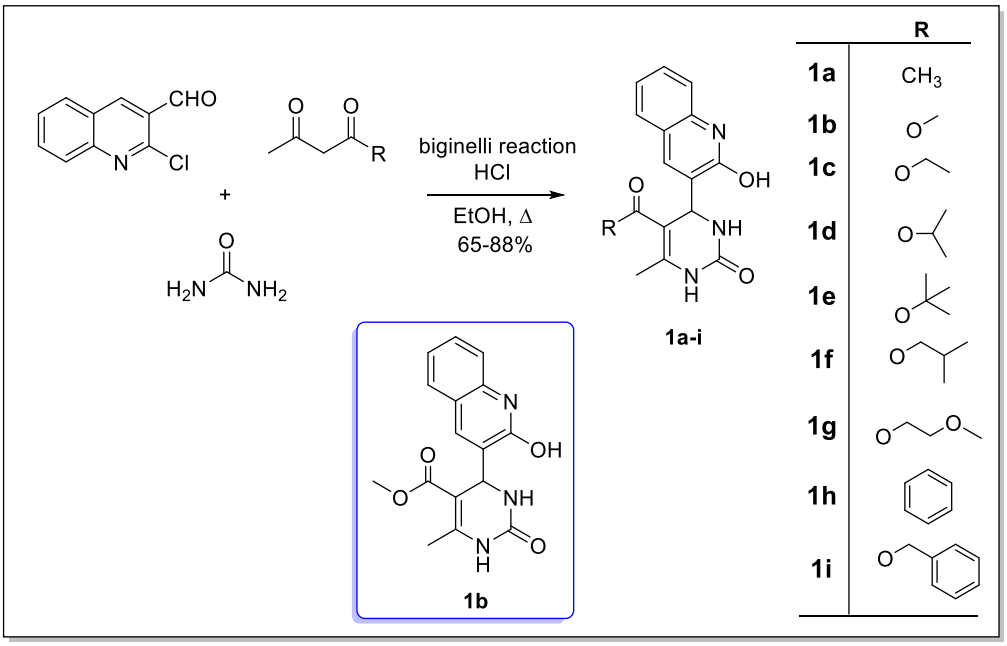

Figure 1. Synthetic Scheme for target derivatives **1a-i**

*Effect of **1b** amount*

The dependence of radiochemical yield on the amount of **1b** is depicted in Figure 2. The reaction was performed at different **1b** amounts (10-300 µg). The radiochemical yield of ^{131}I-**1b** was small at a low **1b** amount where at 10 µg the labeling yield was 62.50 ± 2.50% and by increasing **1b** amount the labeling yield was increased where the maximum labeling yield (96.40 ± 2.20%) was obtained at 200 µg. At **1b** amounts higher than the optimum amount, the labeling yield was slightly decreased again until reached 89.50 ± 2.60% at 300 µg, which may be attributed to the fact that 200 µg of **1b** is enough to capture the entire generated iodonium ion as a result the yield reached a maximum value at this amount.

Effect of CAT amounts

The effect of oxidizing agent amount (CAT) on the labeling efficiency of ^{131}I-**1b** is demonstrated in Figure 3. Radioiodination of **1b** has been performed by using CAT as a mild oxidizing agent, transforming iodide (I^-) to an electropositive form of iodine (oxidative state I^+), which allows a spontaneous electrophilic substitution on the

aromatic ring with a good leaving group such as H^+. When the high specific activity of radioiodide is oxidized *in situ*, it generates electropositive iodine, but it is unlikely to form I_2 because there is so little radioiodine present that statistically it is not possible for two iodine atoms to join together at the concentrations involved (El-Azony, 2010).

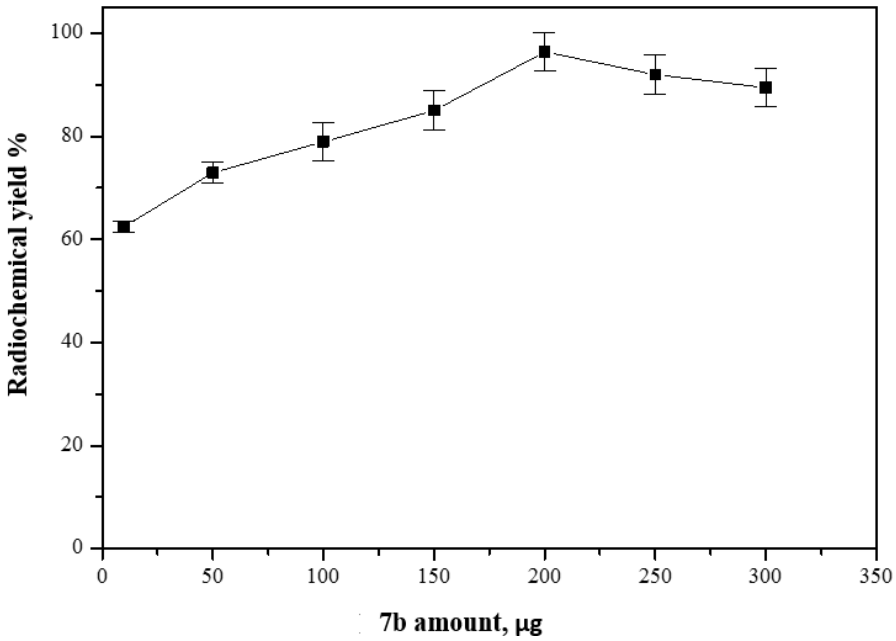

Figure 2. Effect of **1b** amount on the radiochemical yield % of [^{131}I]iodo**1b**

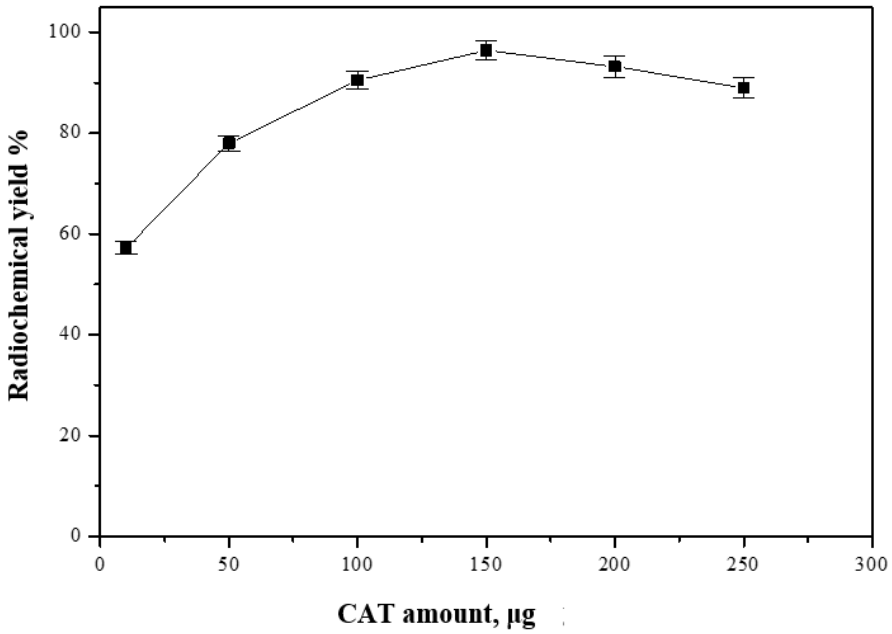

Figure 3. Effect of CAT amount on the radiochemical yield % of ^{131}I-**1b**

In addition, although CAT is a mild oxidizing agent, its effect is enough to oxidize all I^- into I^+ without forming I_2. At low CAT amounts (10 µg), the radiochemical yield of ^{131}I-**1b** was low and equal to 57.20 ± 2.30%. A high radiochemical yield of 96.40 ± 1.90% was achieved by increasing the amount of CAT to 150 µg, increasing the CAT amount above that value led to a slight decrease in the iodination yield where at 250 µg of CAT, the

labeling yield was 89.00 ± 1.90%. This decrease in labeling yield may be attributed to the formation of undesirable oxidative byproducts like chlorination, polymerization, and denaturation of substrate (M. A. Motaleb, Attalah, Shweeta, & Ibrahim, 2023). The formation of these impurities may be attributed to the high reactivity and amount of CAT (El-Rhman, Ibrahim, El-Halim, & El-Tawoosy, 2016). Consequently, the optimum amount of CAT (150 µg) is highly recommended to avoid the formation of by-products and to obtain a high labeling yield.

Effect of pH

Figure 4 shows changing the pH values in the range from 3 up to 10 using buffers to adjust pH at the desired value. The labeling yield for each pH value of the reaction mixture was measured; where at pH 7 the maximum labeling yield (96.40± 1.90%) was obtained and considered the optimum pH. Above and below the pH 7, of the medium led to a decrease in the iodination yield. At pH 10, the labeling yield decreased dramatically to 50.70 ± 1.06% due to an increase in the alkalinity which led to the formation of hypoiodite ion, and at pH 3, the labeling yield was slightly decreased to 89.80 ± 1.09%.

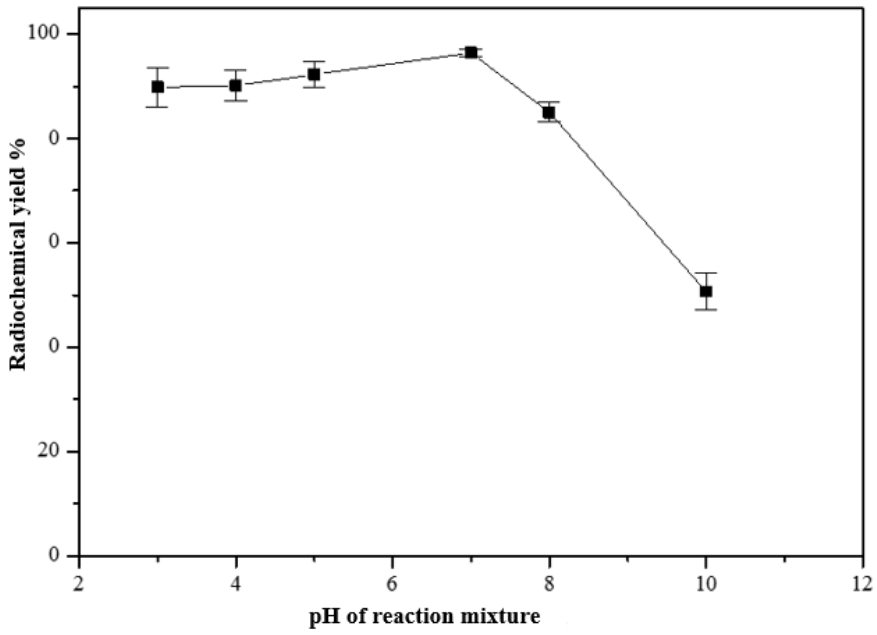

Figure 4. Effect of pH change on the radiochemical yield % of ^{131}I-**1b**

Effect of reaction time

It is clear from Figure 5 that the yield is significantly increased with increasing the reaction time in the range from 5 to 60 min., where at 5 min. The yield was low and by increasing the reaction time the yield was increased till reached its maximum value of 96.40 ± 2.90% at 15 min. *In-vitro* stability of ^{131}I-**1b** was studied in order to determine the suitable time for injection to avoid the formation of the undesired products that result from the radiolysis of the labeled compound. These undesired radioactive products might be accumulated in non-target organs. The results of stability showed that the ^{131}I-**1b** is stable up to 72 h. without detection of any by-products in the reaction mixture affecting the radiochemical yields, thus no significant change in the radiochemical yields was observed.

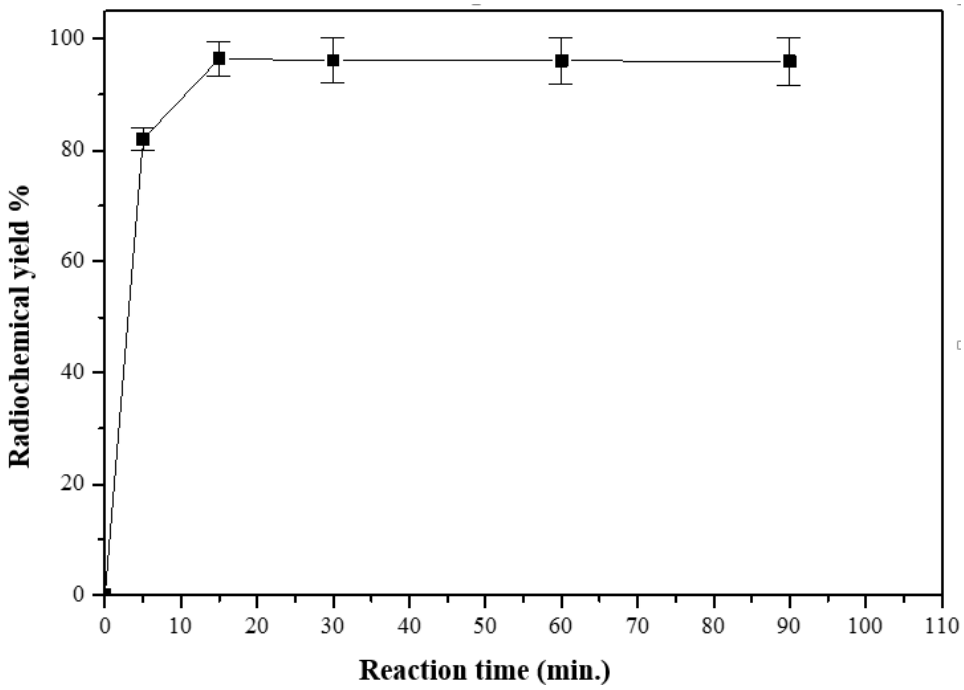

Figure 5. Effect of reaction time on the radiochemical yield % of ^{131}I-**1b**

Table 2. Biodistribution of ^{131}I-**1b** in normal mice

Organs and body fluids	Percent I.D./gram organ /time post-injection, min			
	15	**30**	**60**	**120**
Blood	14.70±1.20	10.3±0.30*	8.25±0.4*	4.2±0.20*
Bone	0.90 ±.01	1.20±0.01*	1.80±0.10*	1.40±0.30*
Muscle	0.70±0.01	0.90±0.02*	1.10±0.021	0.9±0.02
Liver	12.30± 0.5	17.80±0.15*	11.92±0.16*	7.90±0.16*
Lung	2.70±0.10	5.9±0.12*	4.93±0.02*	2.70±0.02*
Heart	5.05±0.05	4.7±0.05	3.50±0.01*	3.20±0.01
Stomach	4.20±0.09	6.3±0.30	4.30±0.16*	3.30±0.16*
Intestine	2.40±0.50	4.40±0.30	5.10±0.9	2.50±0.19*
Kidney (urine)	3.10±0.40	9.30±0.60	15.60±0.30*	24.80±0.30*
Spleen	0.90±0.02	1.60±0.04*	0.80±0.02	0.50±0.02

Values represent mean ± SEM. N=6

*Means significantly differ from the previous value using unpaired student's t-test ($p \leq 0.05$).

3.2. Biodistribution of ^{131}I-1b in normal mice

In normal mice, blood uptake of ^{131}I-**1b** was 14.7% at 15 min post injection and it decreased with time tell reach to 4.2% at 120 min. All tissues showed a decrease in ^{131}I-**1b** uptake within 120 min except kidneys and urine as the

pathway of excretion. Liver uptake of ^{131}I-**1b** with increases may be due to hepatic metabolism. The majority of organs showed a significant decrease in the ^{131}I-**1b** uptake at 120 min post-injection except in the kidney and urine (Table 2).

*Biodistribution of ^{131}I-**1b** in solid tumor-bearing mice*

Table 3 shows the biodistribution of ^{131}I-**1b** in solid tumor-bearing mice. The uptake of ^{131}I-**1b** in the muscle of the right leg (solid tumor) was 3.6, 7.4, 9.3, and 8.9% at 15-, 30-, 60-, and 120 min. post-injection; respectively. The maximum solid tumor uptake was observed after 120 min post-injection of ^{131}I-**1b**. The excretion of ^{131}I-**1b** goes mainly through the urinary pathway. ^{131}I-**1b** uptake in tumor showed higher uptake in tumor cells (T/ NT = 5.0 at 2h post-injection).

Table 3. Biodistribution of ^{131}I-**1b** in solid tumor-bearing mice

Organs and body fluids	Percent I.D./gram organ/time post-injection, min			
	15	**60**	**120**	**240**
Blood	14.70±1.10	12.2±0.02*	6.6±0.04*7	3.5±0.04*
Bone	0.90±0.01	1.20±0.01*	1.40±0.01*	0.80±0.01*
Control muscle	0.90±0.01	0.90±0.02*	0.70±0.002	0.45±0.002
Tumor muscle	2.70±0.01	2.90±0.02*	3.50±0.002	1.75±0.002
Liver	9.30± 0.5	12.80±0.15*	11.92±0.16*	6.90±0.16*
Lung	3.20±0.10	4.92±0.12*	2.4±0.02*	2.30±0.02
Heart	5.5±0.05	5.51±0.05	3.50±0.01*	1.1±0.01*
Stomach	3.70±0.09	5.50±0.30	4.30±0.16*	2.10±0.16*
Intestine	2.40±0.50	5.40±0.30	6.50±0.9*	3.10±0.19*
Kidney (urine)	5.50±0.40	8.04±0.60	16.20±0.30*	21.80±0.30*
Spleen	0.90±0.02	1.60±0.04*	1.20±0.02	0.80±0.02
Normal leg	1.20±0.02	2.80±0.04*	3.10±0.02	3.20±0.02
Tumor leg	3.60±0.40	7.4±0.60	9.30±0.30*	8.90±0.30*

Values represent mean ± SEM. N=6

*Means significantly differ from the previous value using unpaired student's t-test ($p \leq 0.05$).

Target/Non-target ratio

Comparing the uptake of ^{131}I-**1b** in tumor muscle to that in normal muscle (T/NT) was represented in Table 4. The maximum T/NT ratio was 5, obtained at 120 min post-injection. Wash out of ^{131}I-**1b** from normal muscle was

observed rapidly, while the opposite was done in tumor muscle. This may be attributed to that ^{131}I-**1b** may be attached to the DNA of tumor cells.

When uptake of ^{131}I-**1b** in tumor muscle was compared with that of some recently developed radiopharmaceuticals, it was found that it was more than that in most of them as ^{99m}Tc-DMSAme (2.49 at 2 h), ^{99m}Tc-nitride-pyrazolo[1,5-a]pyrimidine (2.2 at 60 min), ^{99m}Tc-BnAO-NI (3.96 at 2 h) and ^{99m}Tc-sunitinib (3 at 1 h) (Table 4).

Table 4. Target/Non target ratio

Time (min)	15	30	60	120
Target/nontarget	2.7/0.9	2,9/0.9	3.5/0.7	1.75/0.45
Ratio	3.0	3.2	5	3.9

Conclusion

Synthesis, radiolabeling, and biological distribution of a novel derivative with radioactive ^{131}I were achieved. The optimum conditions of the labeling of **1b** to give a radiochemical yield of 98.00 ± 2.00% were 200 µg **1b**, 150 µg of CAT, and 150 µL phosphate buffer pH 7 when the reaction mixture was heated at 100 °C for 15 min. A biodistribution study for radioiodinated substrate showed high tumor uptake (8.64 ± 0.02% ID/g at 30 min. p.i.) and a T/NT ratio of 5.17 ± 0.03 at 30 min. p.i. compared with many new tracers that have been developed in recent years. In addition, radioiodinated substrate showed good *in vitro* and *in vivo* stability. So, this research paper demonstrated the possibility of the use of this tracer as an imaging and/or therapeutic agent for cancer. It also encourages further studies on the chemotherapeutic activity of substrate hoping to get a new potent antitumor agent.

Ethics Approval

This work has been approved by the Research Ethics Committee at the Faculty of Pharmacy, Delta University for Science and Technology (FPDU-REC) and holds the approval number FPDU7/2023.

Disclosure

The authors declare no conflict of interest.

References

Abd Elgawad, H., Alhusseiny, S. M., Taman, A., Youssef, M. Y., Mansour, B., Massoud, M., & Handousa, A. (2019). Biological evaluation of newly synthesized quinoline–based compound PPQ-8 in acute and chronic toxoplasmosis: an experimental study. *Experimental parasitology*, *206*, 107756.

Biginelli, C. P. (1893). Aldehyde-urea derivatives of aceto-and oxaloacetic acids. *Gazz. chim. ital*, *23*(1), 360-413.

Bray, F., Ferlay, J., Soerjomataram, I., Siegel, R. L., Torre, L. A., & Jemal, A. (2018). Global cancer statistics 2018: GLOBOCAN estimates of incidence and mortality worldwide for 36 cancers in 185 countries. *CA: a cancer journal for clinicians*, *68*(6), 394-424.

Chu, X.-M., Wang, C., Liu, W., Liang, L.-L., Gong, K.-K., Zhao, C.-Y., & Sun, K.-L. (2019). Quinoline and quinolone dimers and their biological activities: An overview. *European journal of medicinal chemistry*, *161*, 101-117.

Cui, P., Li, X., Zhu, M., Wang, B., Liu, J., & Chen, H. (2017). Design, synthesis and antimicrobial activities of thiouracil derivatives containing triazolo-thiadiazole as SecA inhibitors. *European journal of medicinal chemistry*, *127*, 159-165.

Dawood, D. H., Jasass, R. S., Amin, M. M., Farghaly, T. A., & Abbas, E. M. (2017). Synthesis of Some New Azoloazines with Potent Anti-inflammatory and Analgesic Activity. *Journal of Heterocyclic Chemistry*, *54*(2), 1578-1589.

de Azambuja, G. O., Svetaz, L., Gonçalves, I. L., Corbelini, P. F., von Poser, G. L., Kawano, D. F., ... & Eifler-Lima, V. L. (2019). In vitro antifungal activity of dihydropyrimidinones/thiones against Candida albicans and Cryptococcus neoformans. *Current Bioactive Compounds*, *15*(6), 648-655.

Dobbin, L. (1934). The story of the formula for pyridine. *Journal of Chemical Education, 11*(11), 596. doi:10.1021/ed011p596

El-Azab, A. S., Abdel-Aziz, A. A. M., Ghabbour, H. A., & Al-Gendy, M. A. (2017). Synthesis, in vitro antitumour activity, and molecular docking study of novel 2-substituted mercapto-3-(3, 4, 5-trimethoxybenzyl)-4 (3H)-quinazolinone analogues. *Journal of Enzyme Inhibition and Medicinal Chemistry*, *32*(1), 1229-1239.

El-Azony, K. (2010). Preparation of 125 I-celecoxib with high purity as a possible tumor agent. *Journal of radioanalytical and nuclear chemistry*, *285*(2), 315-320.

El-Barabry, H., Habbak, L., Mansour, B., Youssef, M. Y., Taman, A., & Salem, M. L. (2021). Blocking angiotensin pathway induces anti-fibrotic effects in a mouse model of schistosomiasis by decreasing egg burden and granulomatous reaction. *Egyptian Journal of Cancer and Biomedical Research*, *5*(1), 37-48.

El-Gamal, K. M., El-Morsy, A. M., Sherbini, F. F., Elraheim, A. S. A., Ayaad, R. R., Saad, A. S., ... & Mansour, B. (2022). In vivo Anticonvulsant and Neurotoxicity Evaluation and Docking Study of Promising Novel [1, 5]-Benzodiazepine Derivatives. *Delta University Scientific Journal*, *5*(2).

El-Rhman, M. A. E.-M. A., Ibrahim, I. T., El-Halim, S. M. A., & El-Tawoosy, M. E.-S. (2016). Oxidative radioiodination of meclofenoxate as a preclinical brain imaging agent. *Radiochimica Acta, 104*(7), 491-497.Doi:10.1515/ract-2015-2557

Elblihy, A., Goma, A., Mansour, B., Youssef, M., El Ganyny, G., & Taman, A. (2024). Insights on the therapeutic effect of quinolone-based compound, PPQ-8 plus Nitazoxanide, in chronic toxoplasmosis murine model. *Parasitologists United Journal*, *17*(1), 1-9.

Ergan, E., Akbas, E., Levent, A., Sahin, E., Konus, M., & Seferoglu, N. (2017). Synthesis, theoretical calculation, electrochemistry and total antioxidant capacity of 5-benzoyl-6-phenyl-4-(4-methoxyphenyl)-1, 2, 3, 4-tetrahydro-2-thioxopyrimidine and derivatives. *Journal of Molecular Structure*, *1136*, 231-243.

Fujioka, T., Teramoto, S., Mori, T., Hosokawa, T., Sumida, T., Tominaga, M., & Yabuuchi, Y. (1992). Novel positive inotropic agents: synthesis and biological activities of 6-(3-amino-2-hydroxypropoxy)-2 (1H)-quinolinone derivatives. *Journal of medicinal chemistry*, *35*(20), 3607-3612.

Ghanim, A. M., Girgis, A. S., Kariuki, B. M., Samir, N., Said, M. F., Abdelnaser, A., ... & Panda, S. S. (2022). Design and synthesis of ibuprofen-quinoline conjugates as potential anti-inflammatory and analgesic drug candidates. *Bioorganic chemistry*, *119*, 105557.

Ibrahim, A., Sakr, T., Khoweysa, O., Motaleb, M., Abd El-Bary, A., & El-Kolaly, M. (2015). Radioiodinated anastrozole and epirubicin as potential targeting radiopharmaceuticals for solid tumor imaging. *Journal of Radioanalytical and Nuclear Chemistry, 303*, 967-975.

Kurth, J. M., Dahl, C., & Butt, J. N. (2015). Catalytic Protein Film Electrochemistry Provides a Direct Measure of the Tetrathionate/Thiosulfate Reduction Potential. *Journal of the American Chemical Society, 137*(41), 13232-13235. doi:10.1021/jacs.5b08291

Li, Z. H., Yin, L. Q., Zhao, D. H., Jin, L. H., Sun, Y. J., & Tan, C. (2023). SAR studies of quinoline and derivatives as potential treatments for Alzheimer's disease. *Arabian Journal of Chemistry*, *16*(2), 104502.

Ma, Y., Zhao, S., Ren, Y., Cherukupalli, S., Li, Q., Woodson, M. E., ... & Zhan, P. (2021). Design, synthesis, and evaluation of heteroaryldihydropyrimidine analogues bearing spiro ring as hepatitis B virus capsid protein inhibitors. *European journal of medicinal chemistry*, *225*, 113780.

Mansour, B., Bayoumi, W. A., El-Sayed, M. A., Abouzeid, L. A., & Massoud, M. A. (2022). In vitro cytotoxicity and docking study of novel symmetric and asymmetric dihydropyridines and pyridines as EGFR tyrosine kinase inhibitors. *Chemical biology & drug design, 100*(1), 121-135.

Mansour, B., Henen, M. A., Bayoumi, W. A., El-Sayed, M. A., & Massoud, M. A. (2021). In colorectal cancer; NMR-monitored β-Catenin inhibition by a Quinoline derivative using Water-LOGSY technique. *Journal of Molecular Structure, 1246*, 131151.

Mansour, B., Salem, Y. A., Attallah, K. M., El-Kawy, O. A., Ibrahim, I. T., & Abdel-Aziz, N. I. (2023). Cyanopyridinone-and Cyanopyridine-Based Cancer Cell Pim-1 Inhibitors: Design, Synthesis, Radiolabeling, Biodistribution, and Molecular Modeling Simulation. *ACS omega*, *8*(22), 19351-19366.

Mansour, B. A., El-Sayed, M. A., Massoud, M., & Bayoumi, W. A. (2024). Novel Quinoline-3, 4-dihydropyrimidinone Hybrids Privileged Scaffolds: Design, Synthesis, and Cytotoxic Evaluation. *Delta University Scientific Journal*, *7*(1) 1-8.

Massoud, M. A., El-Sayed, M. A., Bayoumi, W. A., & Mansour, B. (2019). Cytotoxicity and Molecular Targeting Study of Novel 2-Chloro-3-substituted Quinoline Derivatives as Antitumor Agents. *Letters in Drug Design & Discovery, 16*(3), 273-283.

Matada, B. S., Pattanashettar, R., & Yernale, N. G. (2021). A comprehensive review on the biological interest of quinoline and its derivatives. *Bioorganic & Medicinal Chemistry*, *32*, 115973.

Motaleb, M., Abdel-Ghaney, I., Abdel-Bary, H., & Shamsel-Din, H. (2016). Synthesis, radioiodination and biological evaluation of a novel phthalimide derivative. *Journal of Radioanalytical and Nuclear Chemistry, 307*, 363-372.

Motaleb, M., Selim, A. A., El-Tawoosy, M., Sanad, M., & El-Hashash, M. (2017). Synthesis, radiolabeling and biological distribution of a new dioxime derivative as a potential tumor imaging agent. *Journal of Radioanalytical and Nuclear Chemistry, 314*, 1517-1522.

Motaleb, M. A., Attalah, K. M., Shweeta, H. A., & Ibrahim, I. T. (2023). Synthesis and biological evaluation of [131I] iodocarvedilol as a potential radiopharmaceutical for heart imaging. *BMC chemistry*, *17*(1), 21.

Ozaslan, M., Karagoz, I. D., Kilic, I. H., & Guldur, M. E. (2011). Ehrlich ascites carcinoma. *African journal of Biotechnology, 10*(13), 2375-2378.

Patil, P., Padmashal, B., & Uppar, V. Pavankumar H, Eco-Friendly Synthesis of Pyrrolo [1, 2-A] Quinoline Derivatives and Evaluating Their Effects On Hypertension, Inflammation, and Docking Studies.(2023). *Int. J. Life Sci. Pharma Res*, *13*(6), P127-P141.

Ragab, F. A., Abou-Seri, S. M., Abdel-Aziz, S. A., Alfayomy, A. M., & Aboelmagd, M. (2017). Design, synthesis and anticancer activity of new monastrol analogues bearing 1, 3, 4-oxadiazole moiety. *European Journal of Medicinal Chemistry*, *138*, 140-151.

Sakr, T., Essa, B., El-Essawy, F., & El-Mohty, A. (2014). Synthesis and biodistribution of 99 m Tc-PyDA as a potential marker for tumor hypoxia imaging. *Radiochemistry*, *56*, 76-80.

Saleh-Abady, M. M., Naderi-Manesh, H., Alizadeh, A., Shamsipour, F., Balalaie, S., & Arabanian, A. (2010). Anticancer activity of a new gonadotropin releasing hormone analogue. *Biopolymers*, *94*(3), 292-297.

Sharma, S., & Singh, S. (2022). Synthetic routes to quinoline-based derivatives having potential anti-bacterial and anti-fungal properties. *Current Organic Chemistry*, *26*(15), 1453-1469.

Sośnicki, J. G., Struk, Ł., Kurzawski, M., Perużyńska, M., Maciejewska, G., & Droździk, M. (2014). Regioselective synthesis of novel 4, 5-diaryl functionalized 3, 4-dihydropyrimidine-2 (1H)-thiones *via* a non-Biginelli-type approach and evaluation of their in vitro anticancer activity. *Organic & Biomolecular Chemistry*, *12*(21), 3427-3440.

Teleb, M., Zhang, F. X., Farghaly, A. M., Wafa, O. M. A., Fronczek, F. R., Zamponi, G. W., & Fahmy, H. (2017). Synthesis of new N3-substituted dihydropyrimidine derivatives as L-/T-type calcium channel blockers. *European journal of medicinal chemistry*, *134*, 52-61.

Wang, M., Zhang, G., Zhao, J., Cheng, N., Wang, Y., Fu, Y., ... & Wang, Y. (2021). Synthesis and antiviral activity of a series of novel quinoline derivatives as anti-RSV or anti-IAV agents. *European Journal of Medicinal Chemistry*, *214*, 113208.

Xu, J., Yang, J., Ran, Q., Wang, L., Liu, J., Wang, Z., . . . Zhang, L. (2008). Synthesis and biological evaluation of novel 1-O-and 14-O-derivatives of oridonin as potential anticancer drug candidates. *BMCL 18*(16), 4741-4744.

Youssef, A. T., & El Ganyny, G.(2023) Evaluation of the effect of compound ppq-8 combined with nitazoxanide against experimental toxoplasmosis. *Eur. Chem. Bull*. 12(5), 4518-4524.